






Measuring Temperatures Generated by Air Plasma Technology



Cristiano Fragassa^{1*}, Marco Arru², Filippo Capelli¹, Ana Pavlovic¹, Matteo Gherardi¹

¹ Department of Industrial Engineering, University of Bologna, 40136 Bologna, Italy

² Ardesia Technologies S.r.l., 40055 Villanova di Castenaso, Italy

* Correspondence: Cristiano Fragassa (cristiano.fragassa@unibo.it)

Received: 08-26-2022

Revised: 09-15-2022

Accepted: 10-06-2022

Citation: C. Fragassa, M. Arru, F. Capelli, A. Pavlovic, and M. Gherardi, "Measuring temperatures generated by air plasma technology," *Power Eng. Eng. Thermophys.*, vol. 1, no. 1, pp. 76-91, 2022. <https://doi.org/10.56578/peet010108>.



© 2022 by the authors. Licensee Acadlore Publishing Services Limited, Hong Kong. This article can be downloaded for free, and reused and quoted with a citation of the original published version, under the CC BY 4.0 license.

Abstract: The atmospheric pressure air plasma technology is based on the general principle of transforming the air into an ideal conductor of plasma energy thanks to the application of an electric potential difference able to ionize the molecules. Applying the principle to the human surgery, it comes to be possible to assure an energy transfer from plasma-generator devices to the human tissue in a relatively simple way: passing through the air, with exceptionally limited effects in terms of tissue heating. Such a condition is very useful to assure effective treatments in surgery: less thermal damage, fewer side effects on the patient. This is also what emerged during the use of innovative devices embedding the Airplasma® technology (by Otech Industry S.r.l.), where temperatures on human tissues were measured stably below 50°C. However, the profiles assumed by the temperature along the different electrodes during the operating conditions are rather unclear. This knowledge is essential to improve the efficiency of the electrodes (through their redesign in shapes and materials) as well as to reduce the invasiveness of surgical interventions. The present work had the purpose of characterizing the most common electrodes thanks to temperature measurements carried out by infrared sensors respect to different operating conditions. A simplified finite element model was also developed to support the optimal redesign of electrodes.

Keywords: Atmospheric pressure plasma; Temperature measurement; IR sensors; Human surgery; Air plasma

1. Introduction

The human surgical practice has very ancient origins, lost in the mists of time, but always shown itself to be very attentive to grab every opportunity of improvement deriving from the most advanced engineering innovation.

It began when man realized that he could intervene on malfunctioning anatomical structures with cutting tools, improving or even saving the lives of patients. Its evolution has been constant [1] with a decisive leap forward with the discovery of sepsis, the sterilization of instruments [2] and surgical anesthesia [3].

A further problem in surgical practice is hemorrhage as the cut inevitably causes the cutting of blood vessels with relative blood loss. Bleeding has two negative effects:

- 1) cause exsanguination of the patient through the copious loss of blood
- 2) make the operation difficult due to the blood that prevents the vision of the anatomical structures

Several tricks point to cauterizing blood vessels using temperature [4].

Electrosurgery was born precisely to allow controlled cutting and cauterization. Electrosurgical units treat the patient's body as a resistance. Through electrical diathermy they raise the temperature at the point where the electrode is in contact and induce ablation, tissue cutting and tissue cauterization with consequent haemostasis.

The first use reported in the literature of diathermic surgical instruments dates to the second half of the 1800s by J. Marshal (1818 - 1891), later popularized by W.T. Bovie (1882–1958) between 1914 and 1927 [5], not without some perplexities related to the onset of complications of post-surgical healing [6, 7]. These undesirable effects are to be attributed precisely to the type of action of electrical diathermy which blocks hemostasis by upsetting the anatomy of the tissues, but also makes them unable to effectively implement the regeneration and healing processes. This can result in unsightly scarring, suture dehiscence, and other surgical wound healing problems.

Other instruments have also been developed more recently than the electrosurgical unit. The surgical laser was

first used in surgery in 1962 for the removal of atherosclerotic plaques by Mr. Paul E. McGuff [8]. The broadest development in the surgical field will only take place around the 70s and 80s [9]. The laser finds applications in soft tissues where the energy of the light in the form of photons excites the water molecules causing vaporization of the tissues. Thus, it can be used for both surface ablation and tissue cutting. The laser also induces hemostasis in vessels up to 2 mm in size. The laser is mainly used in skin surgery, oropharyngeal surgery, ear surgery, eye surgery and gynecology. So, in districts that are easily accessible from the outside. The laser requires important precautions, such as the careful preparation of the operating field and of the operators to prevent the laser light from reaching dangerous targets: tracheo-tubes with oxygen, the operators' eyes and any flammable material. The laser causes less tissue damage than the electrosurgical unit, reducing post-surgical complications. At the end of the past millennium, in the wake of the electrosurgical unit, a new technology was developed which is based on the rapid alternation of electrical energy (radiofrequency scalpel). The principle of tissue vaporization, unlike the electrosurgical unit, is not based on heat, but on the excitation and ionization of the water molecules present in the tissue which, crossed by these high-frequency alternating currents, change state from liquid to they turn into steam. This system allows to obtain a result similar to the electrosurgical unit, with a lower temperature (between 70 and 100°C), a lateral damage of a few hundreds of microns against a damage of a few mm induced by the electrosurgical unit [10].

However, these techniques involve the use of electric fields in the patient's body, but for some it can be a problem (pacemaker carriers, subject to cardiac arrhythmias).

Another way is that of ultrasound: the energy localized inside a forceps causes the denaturation of proteins, the dissection of tissues and the sealing of vessels. This energy is generated by electrical impulses and changes in the nature of the molecules (ionization or evaporation), by the kinetic energy determined by the vibrations which upset the anatomical structure of the tissues [11]. This technology practically induces a thermal alteration of the tissues in the area surrounding the action of the device, consequences on the healing of the treated area.

The use of ultrasound is limited in districts where it is possible to intervene with pincer-shaped devices and cannot be used in the case of precision and fine-cut interventions. On the other hand, it is a technology that can be used in micro-invasive surgery, allowing for laparoscopic surgery. A similar application is performed by Ligasure®, an instrument that combines mechanical pressure exerted by a clamp with bipolar-type radiofrequency energy transmitted between the two electrodes inducing changes in the anatomical tissue structures and sealing of the vessels. Lateral tissue damage is rather reduced, promoting healing of the treated areas [12]. Ligasure® was created to cauterize and its surgical use is rather limited (in situations where you intend to cut flaps or where you intend to seal intra-abdominal structures in laparoscopic procedures) [13].

Compared to this panorama, an innovation in precision electrosurgery that deserves attention is represented by the so-called air plasma technology [14-22]. Throughout the ionization of the molecules in the air, atmospheric pressure air plasma technology allows the generation of a stable flow of plasma at environmental conditions of temperature and pressure. And its potential uses are manifold [1]. In surgery, e.g., using a 'cold plasma' makes possible to get precise and minimally invasive incisions on skin and tissues. Thus, the surgical incisions are clear and decisive, little different from those of the surgeon's blade and at the same time without the burns typical of electrosurgical units. Several experiments have confirmed its medical validity over the years by promoting the spread of cold plasma as alternative in surgery [2].

Referred to as CAPP (from Cold Atmospheric Pressure Plasma) in surgical manuals also, atmospheric pressure air plasma intervenes by reducing bleeding just like traditional electrosurgery, but with less thermal damage of tissues. Three consequent advantages make such an unconventional technology interesting in surgery: a) reduction of post-operative pain; b) faster healing of wounds; c) better functional and aesthetic result.

However, there are still not many devices that use this technology in electrosurgery. The most popular is probably the Peak Plasmablade®, a high-frequency monopolar device that uses the alternating potential energy developed to cut with the blade touching the tissue, but also with the creation of plasma (ionized gas) between the electrode and the patient [3]. It thus proves capable of producing cutting and hemostasis at a lower temperature (between 40 and 100°C) than conventional electrosurgery. However, this temperature makes it possible to seal small vessels and produce hemostasis [4].

Airplasma®, the different technology on which this study is focused, is a patented cold plasma technology [5] for surgical purposes developed and marketed by Otech Industry S.r.l., and recently embedded in the creation of medical-surgical devices for human and veterinary surgery. It is based on the principle of creating a flow of plasma in the air by an ionization process without additional gases, to be used it for different scopes in human and veterinary surgery. Specifically, Airplasma® is currently applied in surgery and aesthetic medicine, through the Oneyonis® device on humans [6] and Onemytis® device on animals [7]. The passage of energy from these devices to the tissue occurs through the air as a means of transmission and with a dissipation temperature on the tissues which, according to the first tests carried out through a thermal imaging camera, always appears to remain below 50 °C. Several clinical investigations provide evidence of the usability of Airplasma® technology [8].

Hence the name of 'cold plasma' and many of its interesting functional properties that are supporting the rapid spread of the technology in clinical practice. For this purpose, with Airplasma® a wide range of scalpels is already

available, different from each other in shapes and materials, able to best adapt to the different needs of the surgeon.

Regarding such scalpels, the profiles assumed by the temperature in these electrodes during the operating conditions are still unclear and deserve to be investigated. In fact, this information is essential for various purposes that converge in the general concept of moving towards a better understanding of how technology works.

Through a more accurate understanding of the thermal-dynamic behavior of the scalpel, followed by an adequate data-driven design, it would be possible, for instance, to make improvements to the surgical devices. It is possible, e.g., to imagine the general lowering of the temperatures present which would lead to (further) reducing the thermal effect on the tissue, but also to optimizing devices' consumption.

Hence the need to thermally characterize the electrodes during their operating conditions emerges. The present study describes the way such characterization was experimentally performed, proposing its main results in terms of temperatures. A simplified numerical model, based on finite elements, was also presented as a way to support the optimal redesign of more effective electrodes.

2. Methodology

2.1 Scalpels

Four scalpels/electrodes for Oneyonis®, characterized by relevant differences in geometry and materials, were here considered, as represented in Table 1 and Figure 1. These scalpels have been used for some time by surgeons and represent the most common in the clinical setting. at the same time, their characteristics are such as to represent a useful test bed for the investigation.

Table 1. Different surgery electrodes under consideration

Code	Shape	Material	Length [mm]	Diameter [mm]
ESST1	straight tip	steel	28	0.8
ESTT1	straight tip	tungsten	24	0.3
ESSP4	spatula	steel	20	2.0
ESSH3	ball	steel	20	3.0

Specifically, while the scalpel called ESST1 is represented, in practice, by a long steel tip, the ESTT1 is very similar, but with a large part of the tip coated in Teflon. The presence of Teflon allows an electrical and thermal insulation which reduces the risk of uncontrolled electrical discharges (because not on the extremity), as well as accidental thermal contact between the scalpel and the patient's tissues (which could cause unnecessary burns). Both scalpels are perfect for very high precision cuts, given the very sharp edges. Scalpels ESSP\$ and ESSH3, characterized by an extremity of larger and well-defined geometric shape, respectively a spatula and a sphere, are used for different operations, such as removal of diseased tissues and ablations. On the one hand, these shapes appear less critical than the sharp ones (lacking a 'spike effect'), on the other hand they offer wider geometries, whose influences on the functions of the scalpel deserve to be studied.



Figure 1. Different geometries of electrodes under consideration: (a) straight tip in steel; (b) straight tip in tungsten; (c) spatula; (d) ball

2.2 Equipment

Tests were performed using:

- two IROPTRIS thermal probes, low range (-50°C - 975°C) and high range (250°C - 1,800°C)
- two Mc Pearson current probes
- one Tektronix high voltage probe (20 kV)
- one Tektronix MSO46 oscilloscope

- a thermocouple
- a stirrer heating plate

Furthermore, a specially positioning device was designed and manufactured, merging rapid prototyping parts to aluminum profiles, in the way to ensure accuracy in measurements (Figure 2).

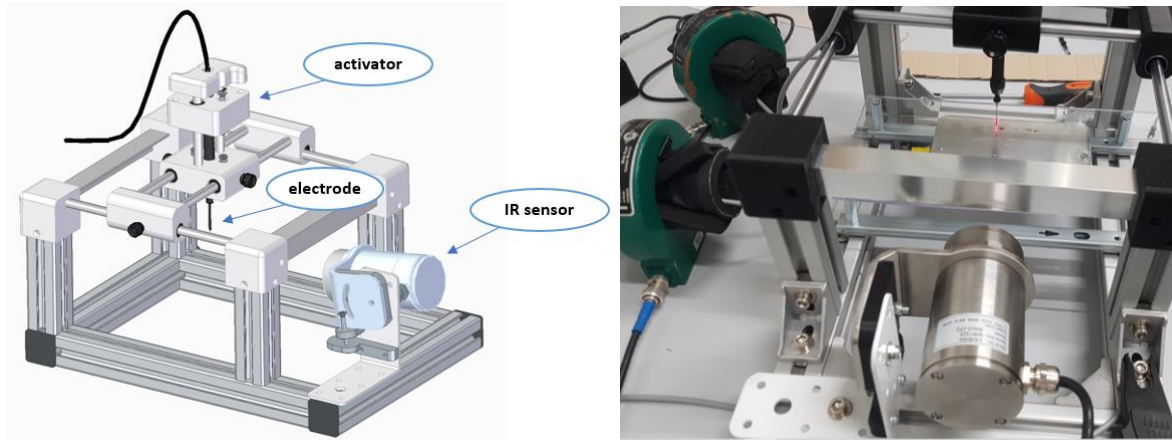


Figure 2. Overview of the experimental equipment

2.3 Preliminary Activity

Preliminary tests aimed at identifying the emissivity coefficients with respect to the different materials: this is essential to be able to obtain absolute values of temperatures from data collected by the IR thermal probes.

Following the recommended procedures, two of the electrodes were used, heated to 100°C by contact on a heating plate, simultaneously measuring the temperature of the plate by thermocouple and of the electrode by means of an IR thermal probe (low temperature IR probe was used). Tests were repeated for each of the materials of interest. The measured values were verified in line with those of the literature (Table 2).

Table 2. Emissivity of materials under consideration

Material	Emissivity
Steel	0.16
Tungsten	0.20
Teflon	0.68

Practically, a reparameterization factor (per each material) was measured in this way, which the software uses to allow working with the IR probes either in terms of emissivity or temperatures. This factor relates to a single parameterization / calibration point, chosen in the case equal to 100°C, based on the assumption (in line with physical considerations) of a linear proportionality between emissivity and temperature of a course (in the range of measurements of our interest). This assumption was then rechecked by comparing (in the case of steel only) the 'reading' of temperatures by means of a probe and by means of a thermocouple for a heating ramp (66 -> 246°C), with values from the Table 3.

Table 3. Comparison between the temperatures measured by thermocouple and IR probe

Thermocouple	IR probe	Delta
66	66	0,0%
100	100	0,0%
108	109	1,5%
157	155	-3,0%
165	164	-1,5%
246	244	-3,0%

Although there are apparently non-marginal differences (3%), this occurs only at a specific level and is linked to external factors that are difficult to control (thermal inertia and decimal truncations in the measurements). On the contrary, the correlation between the measures is in fact practically perfect, as evident in Figure 3 and by a correlation coefficient (Pearson) of 0.99993.

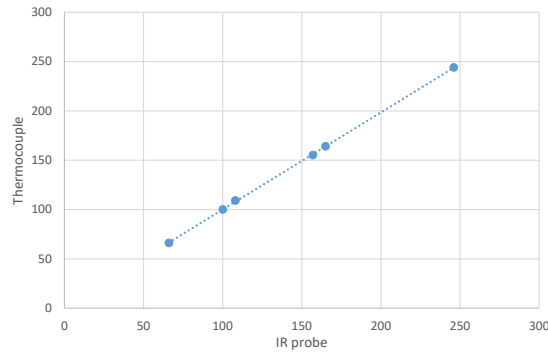


Figure 3. Linearity between the temperatures measured by thermocouple and IR probe

2.4 Equipment Installation

The experimental mock-up, in Figure 4, was assembled by the following steps:

- placed the positioning device on the workbench
- connected the discharge plate
- connected the discharge plate to a resistive load of $23K\Omega$
- connected high voltage probe to the electrode head
- installed the current probe on the cable of the handpiece (input current)
- installed the current probe on the stabilizer cable (output current)

Then, preliminary tests were performed with the scope to verify the experimental mock-up usability and limits.

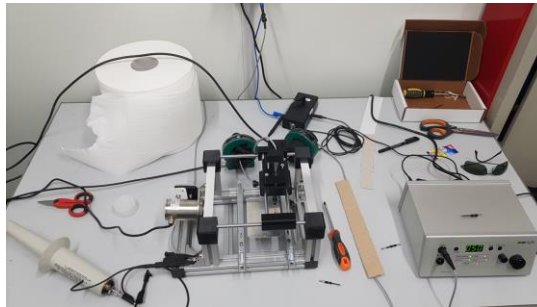


Figure 4. Experimental mock-up

As first, the chance of limiting the experiment to the use of the LOW IR probe was investigated.

Preliminary measurements showed that temperatures used to stay under 700°C , during tests. Then they were acceptably below the maximum scale of the probe ($= 975^{\circ}\text{C}$) and this happened whenever a resistance was applied. It was practically represented by maintaining a certain distance of the electrode from the plate.

On the contrary, it was also evident that in conditions close to the short circuits, the temperature rapidly rose (over $1,200^{\circ}\text{C}$) not allowing the use of the LOW IR probe. Unfortunately, it also emerged that the most interesting values of temperatures seemed to stay around $900\text{-}1000$ degrees, which is precisely the limit of the LOW IR probe.

Then, tests were carried out using the HIGH IR probe with measures in the range of $250\text{-}1800^{\circ}\text{C}$. The use of a single probe helped to minimize experimental errors, reducing changes in equipment configurations, which would impact on the measurement accuracy. At the same time, this choice also meant that below 250°C there was no measurement while all temperature profiles were recorded starting from 250°C .

2.5 Preliminary Configurations

With the scope of assuring the identical testing conditions to each electrode under investigation, changes in the experimental configuration were sometimes needed with respect to the geometric characteristics of the electrodes, such as:

2.5.1 Distance between electrode and substrate

The positioning equipment allowed the electrode to be mechanically lowered to bring it to touch, thus igniting the plasma arc in the air. A spring system then moved the electrode back to the starting position. The gap between electrode and substrate was one main parameter characterizing the experiment. This distance, in fact, represents

the thickness of the dielectric (air) necessary to break and maintain in a plasma state through the discharge between the electrode and the substrate (which in all the tests consisted of a metal plane). For electrodes ESST1 and ESTT1 the distance was set to 1.2 mm, then modified to 0.7-0.8 for the other ones.

2.5.2 Measurement points

The IR probe permitted to deliver a local measurement of temperature respect to a specific target point. For this it was very important to define the measuring points precisely. Moreover, the purpose of the work was to detect these temperatures in a reasonable number of points in the way to define an experimental profile respect to each electrode of interest, but also in the way to use this information as a basis for developing a numerical model.

Table 4 and Figure 5 detail the number and position of points that were considered during tests: they were labelled as A, B, C and D according to the progressive distance from the substrate / scalpel's extremity. As far as possible the distances between the points remained around 2mm. Lower distances between the measuring points were not considered as they were difficult to be evaluated in terms of accuracy with the available equipment. As a result, only the ESST1 and ESTT1 scalpels have more measurement points related to the metal background (measurements on Teflon, as will be seen, present inconsistencies and, therefore, were limited).

Table 4. Number of measuring points and their distance from the substrate

Electrode	Points	Distance (mm)
ESST1	4	1.2
ESTT1	3	1.2
ESSP4	1	0.7
ESSH3	1	0.8

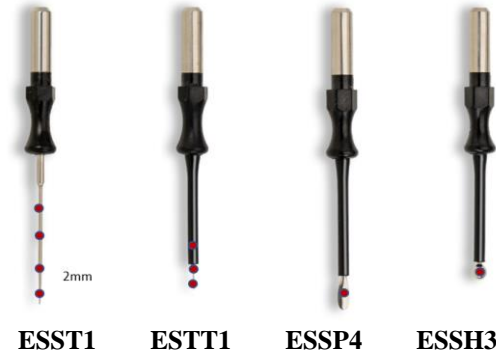


Figure 5. Visual representation of the measuring points for the different electrodes

During test, the current intensity was kept as stable as possible, modulating, instead, the voltage through a specific knob, respect to at specific thresholds (100% - 70% - 40%). The value of intensity was checked (almost) on all tests, observing the current trend and recording the maximum value (excluding spurious peaks). The value of potential, which could not be checked during the test, was validated occasionally (to reduce the risk of changing the general system settings). During the experiments, the current intensity had a value of 2.38 ± 0.26 A, which is equivalent to a range of variation of 0.52A, equal to about $\pm 21.8\%$. The potential was generally stable.

2.5.3 Measurement conditions

Tests were carried out taking into account:

- 4 electrodes' geometry (namely ESST1, ESTT1, ESSP4 and ESSH3)
- 3 electrodes' materials (steel, tungsten, Teflon)
- 2 substrates (primarily steel, but also organic tissue was also used once)
- 3 current intensities (100% - 70% - 40% of maximum values).
- 4 measurement points (namely A, B, C, D at a progressive distance from the substrate)

for a total of 288 potential conditions, of which 65 combinations (22.5%) were really investigated.

With the need to have a statistical basis, measurements were repeated three times, at least, measuring the trends over time of current intensity (A) and temperature ($^{\circ}\text{C}$).

3. Results and Discussion

Each test was carried out by igniting the plasma by applying a certain electric potential and observing the temperature increase at a specific point of a specific scalpel until reaching a plateau condition that defines the

maximum temperature. Experimental results are summarized in *Appendix A* where relevant information such as electrode type, point of measurement, current intensity (A) and level (%), test duration (s), maximum temperature (°C) were reported respect to each test.

3.1 Temperature Profiles

Figure 6 shows a characteristic trend of temperatures over time, as measured by the IR probe. As expected, an increase is evident with a linear trend at the beginning followed by a stabilization plateau. The presence of such plateau was used to obtain the comparison parameters of Maximum Temperature (T_{max} in °C) and Time (t in sec.)

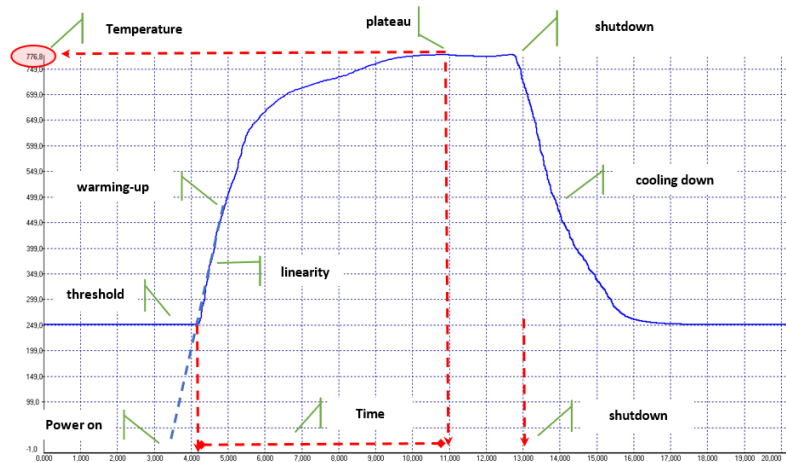


Figure 6. Representative temperature profile with main information

3.1.1 Plateau

The plateau was commonly reached between 5 to 20 sec. With respect to this time, it must be also considered how, given the fact that IR HIGH probe was not able to detect anything below the threshold of 250°C, this value should be improved by the period necessary for the electrode to reach the 250°C (from the room temperature). Moreover, no information was available regarding what happened at lower temperatures (<250°C). However, this fact has no particular effect on the study's relevance since:

- the metal parts of the electrode exceeded 250°C in just a few seconds (4-5 sec)
- the electrode extremity exceeded this threshold in less than one second
- the electrode is designed to be used in a stationary / slowly variable thermal situation
- during the surgeon's operations, greater dissipative loads slow down non-stationary phenomena.

Basically, what we are looking at thanks to the present experiment can be thought of as the worst possible configuration with continuous generation. In practice such condition never happens. Furthermore, the metal plate on which we turned on the instrument causes a much faster heating of the electrode than the tissue.

Better investigating this situation, it is possible to say that, in the case of the ESST1 electrode, the heating from 250°C to the maximum value was 7.7 (A), 8.0 (B), 9.6 (C) or 12.3 (D) sec depending on the specific point of measurement. It was also evident how the extreme areas of the electrode (point A and B) reach equilibrium quickly (8 seconds, 30% before point D), and how they did it almost simultaneously. On a practical level, this difference in the heating rate between the different points of the electrode (4 sec between A and D) is completely negligible (Figure 7).

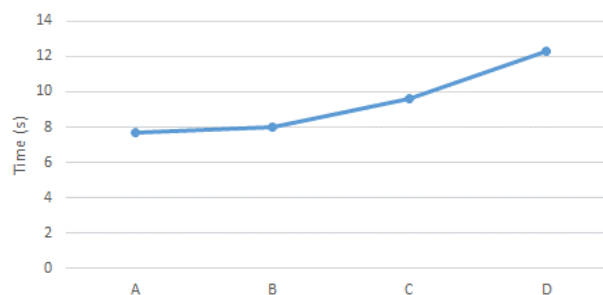


Figure 7. Speed of reaching thermal equilibrium in the different points for an electrode

3.1.2 Continuous growth

Unfortunately, some measurements showed a continuous growth, without an evident plateau, with a rapid rise in the first period progressively slowed down (Figure 8). In the case, the experiment was interrupted before a stabilization of the temperature (anticipated shutdown). Not being able to detect a maximum, the temperature at a reference time (chosen as 22 sec from ignition) was considered.

Trends without plateaus emerged in the case of Teflon coated electrodes: the Teflon acted by gradually heating up the electrode, slowed down the arrival of the metal electrode to thermal saturation. In the case, the tests were stopped because the Teflon started to emit smoke, proving to be very close to its melting temperature (327°C).

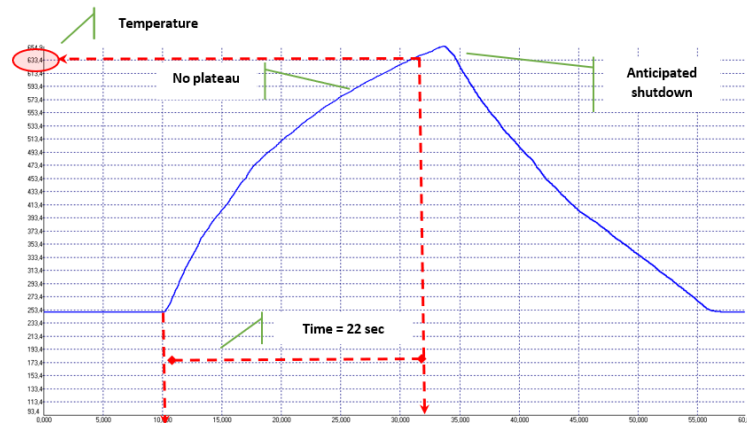


Figure 8. Example of temperature profile measured without plateau

3.1.3 Substrate

The tests were originally designed to be carried out with respect to two substrates:

- metal steel
- organic tissue (i.e., chicken meat)

Regarding the metal plate as substrate, preliminary tests made it clear that the (short circuit) contact between the electrodes the plate did not create conditions of interest to be investigated. Aside from the fact it is not representative of the normal use of the surgical scalpel, what happens is also rather trivial: the plasma in air is not activated and the electrode heated only by the joule effect.

Regarding the organic tissue as substrate, even if some preliminary tests were carried out, they were only able to demonstrate their complexity. Specifically, they are poor in terms of repeatability of the measurements and, then, they were suspended due to the evident impossibility of obtaining useful results. There are several problems that emerge during these experiments, mainly related to the fact that it is not possible to keep the plasma on the same point for more than a few moments. The organic tissue is, in fact, immediately sublimated (by evaporation, since the plasma has been designed for this purpose) and the conditions of the substrate are quickly modified (making the stability and repeatability of the measurement difficult).

Respect to further experiments, some changes can be here proposed, such as the introduction of:

- a trolley slowly moving the substrate relative to the plasma
- a plexiglass cover/mask able to press and uniform in thickness the tissue with a hole through which the plasma is applied, better if performed under an experiment hood.

Tests, therefore, were focused on metal substrate and electrode without direct contact (as in Figure 9).

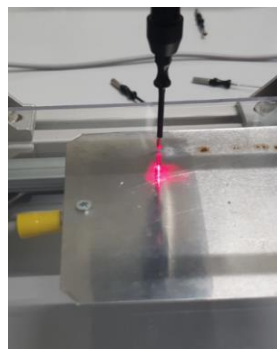


Figure 9. Experimental setup made by electrode and metal sheet, without a physical contact

3.2 Preliminary Results

Several aspects and considerations preliminary emerged from results.

3.2.1 Preliminary feedbacks

Initial tests (numbered from 1 to 5) showed very fluctuating measurements. It was unexpected. After a check, a probe misalignment was found. The measurements themselves were ignored, but the situation made clear that:

- The probe had the ability to be very precise. It offered very strictly localized measurements confirming the possibility of using such measuring instrument in terms of accuracy.
- The tests must be carried out paying attention in the alignments and minimizing all unnecessary system movements / modifications. This confirmed the methodological choices to: -) limit the use of IR sensors to one probe (instead of two) for all measurements; -) avoid measuring the potential too often. Otherwise, such additional information would not have added much, at the same time making the measurements less understandable due to the risk of introducing recalibration errors.

3.2.2 Plasma

Tests N. 6-9, carried out on the electrode but in a location very close to the plasma (A), showed an out-of-scale temperature ($> 1,800^{\circ}\text{C}$), except in the case of a test which reports a temperature of $1,764^{\circ}\text{C}$. This fact suggested that the plasma could be at temperatures of the order of $1,800^{\circ}\text{C}$. Such indirect information is useful, especially considering that there was no way to directly detect the plasma temperature by the experimental system (the IR probes). It was not only due to out-of-scale values, but also since the plasma emissivity parameters were missing and very difficult to be estimated. Finally, the measurement may have been disturbed by the effect of plasma presence intended in terms of obscuring the emissivity of the metallic electrode. However, such high temperatures could be also indirectly confirmed by the slow but progressive wear of the metal scalpels (not present in the case of tungsten scalpels). The only reason can be related to the fact that some areas of the metallic electrodes reach temperatures higher than those of steel melting ($1400\text{-}1500^{\circ}\text{C}$), but well below that of tungsten ($3,422^{\circ}\text{C}$).

3.2.3 Thermal fatigue

Tests N. 6 - 9, carried out moving away from the plasma (point B), indicated a lower temperature, of the order of $930\text{-}1085^{\circ}\text{C}$. Rapid cooling of the material was then confirmed ($700\text{-}800^{\circ}\text{C}$ / 2mm). Microstructure considerations should be made in electrodes' design in relation to differentiated expansion and low cycle thermal fatigue. This aspect can be even more relevant in the case of areas where different materials (e.g., steel / tungsten) are jointed.

3.2.4 Accuracy

Tests No. 10 - 18, carried out still away from the plasma, continued to indicate a rapid drop in temperature, now in the range $547\text{-}662^{\circ}\text{C}$. Furthermore, having repeated the measurement 6 times, allows for 618 ± 42 , which represents $\pm 7\%$. The accuracy in measurements was generally confirmed, even after further rechecks, to be around a variability of $\pm 7\text{-}10\%$, therefore suitable for this type of study.

3.2.5 Repeatability

A caution was raised with respect to the rapid deterioration of the electrodes. This situation, which originates a change in their geometry and in the material surface property (e.g., due to oxidation), could represent one of the reasons for the results' variability. In this specific case, the electrodes were often cleaned and realigned. At the same time, attempts were made to observe any 'degrading' trends in temperature values, with increases / decreases, instead of the causal oscillations typical of measurement errors. Considering results, as in Figure 10, degradation phenomenon could not be excluded, but was not significant.

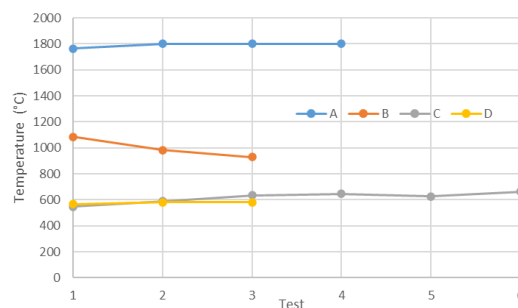


Figure 10. Example of the trend of the measures that demonstrates their certain stability over time

3.2.6 Intensity

Special attention was paid to verifying the effect of modifications in the current intensity over the temperature. Changes were carried out by means of a knob with respect to the three reference values of 100%, 70%, 40% corresponding to, respectively, 2.52, 2.37, 2.29 A of intensity. Figure 11 reports these results.

A linear correspondence between Intensity vs Current emerged, with linearity of 0.98. The temperature showed a weakly linear inverse trend (-0.46): increasing the intensity seems to decrease slightly.

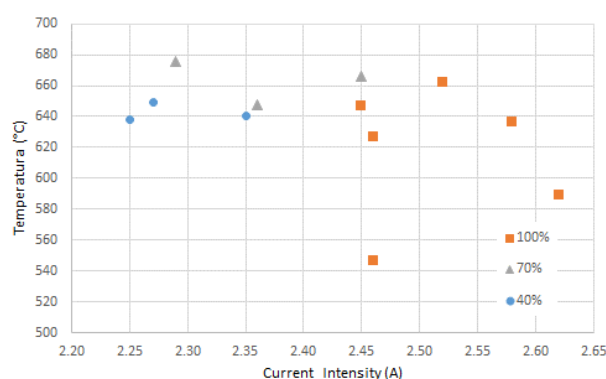


Figure 11. Investigating the effect of current intensity and potential over the temperature

3.2.7 Teflon

The measurement on the Teflon coat (i.e., ESSP4 scalpel, point C) highlighted the function of reducing the temperature with respect to the metal substrate, reduced by about 100-150°C, and therefore to correctly act as a protection. However, it still remained at rather high temperatures (at 373°C), above those that would cause burns, as well as above the melting point of the material. The prolonged use (> 20 sec) of the scalpel under load conditions similar to those of the test can act 'burning' the Teflon (the tests were interrupted due to the emission of strong odors). This situation contributed to creating a progressive heat accumulation effect in the scalpel, favored by: a) greater mass; b) presence of an insulator that opposes the heat dissipation; c) Teflon melting. Once turned off, the scalpel takes much longer to cool down.

3.3 Comparative Measures

Table 5 and Figure 12 report a summary of the measured temperature, expressed as an average of 3 or more measures, for each of the four electrodes under investigation, with respect to (up to) 4 points under analysis (about 2 mm away from each other) and considering the three current intensity / potential levels. It is clearly observable (again) that the intensity of the current did not affect the temperature. On the contrary, it is also evident / confirmed how temperatures were significantly modified by changes in electrodes' geometry and distance from the plasma.

Table 5. Temperatures for different conditions

Electrode	Material	Point	100%	70%	40%
ESST1	Steel	A	1620		
ESST1	Steel	B	999		
ESST1	Steel	C	618	663	642
ESST1	Steel	D	576	572	550
ESTT1	Tungsten	A	1226		
ESTT1	Steel	B	641	653	627
ESSP4	Steel	A	1013	1021	1017
ESSP4	Steel	B	608	607	600
ESSP4	Teflon	C	373		
ESSH3	Steel	A	642	645	643

Specifically, comparing temperatures in terms of their average values, it emerges or returns to emerge as:

- The current intensity did not substantially affect the electrode temperature, for any of the points.
- There was an immediate drop in temperatures with moving away from the electrode extremity. It is possible to estimate such decrease as 200 - 300°C / mm passing between points A -> B, and 100 - 150°C / mm from B -> C (with 2 mm between A and B or between B and C.).
- The gap in temperature was approximately the same between points and between electrodes when it is

examined as percentage (%): passing from A -> B -> C, the temperature drops by about 20-25% / mm regardless of the specific electrode. It is evident comparing diagrams in Figure 13 and suggests the possibility of developing rather accurate physical or numerical models.

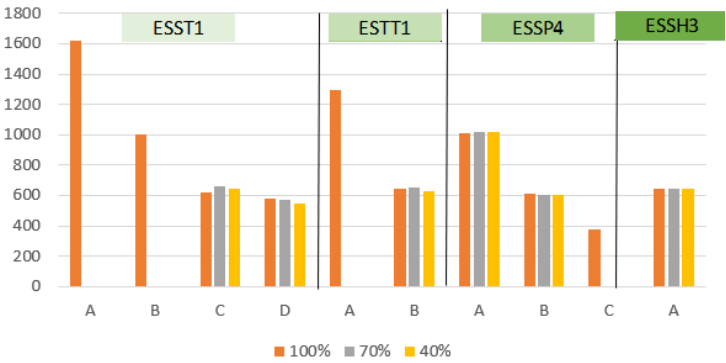


Figure 12. Temperature vs intensity for different points and electrodes



Figure 13. Temperature drop when moving away from the plasma area, in (a) absolute and (b) % values

Figure 14 reports representative trends of temperatures in the case of different electrodes. This is very useful for an immediate comparison of their different thermal behavior.

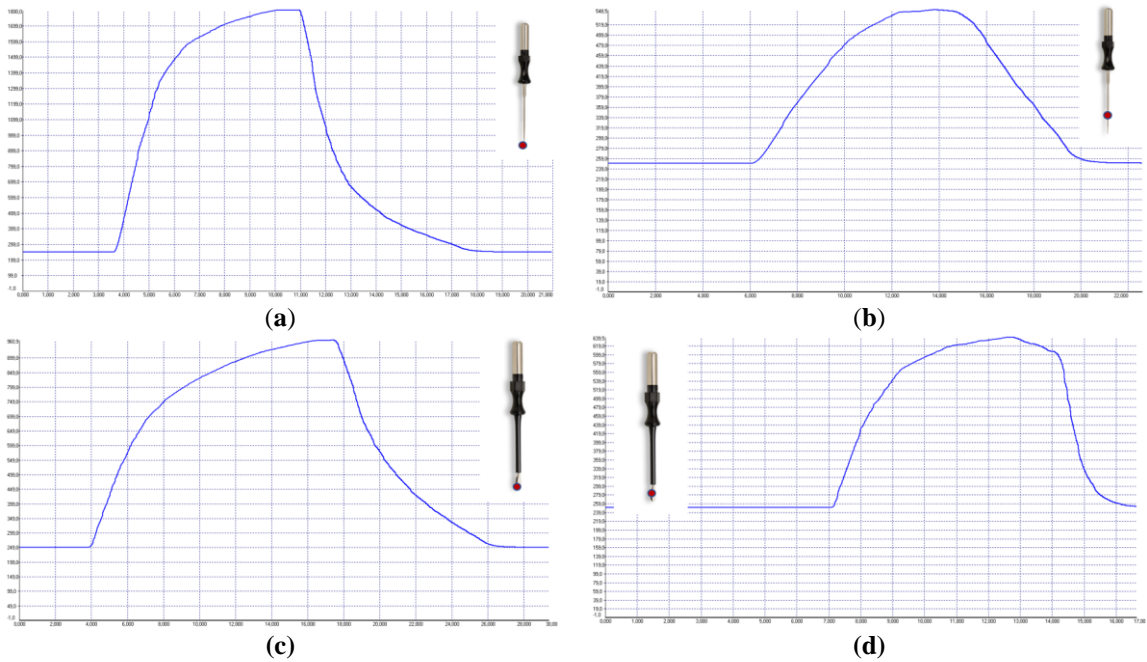


Figure 14. Trend of temperatures in the case of different electrodes: (a) at the tip of the steel electrode; (b) at 4 mm from the tip; (c) steel spatula; (d) at 2 mm for steel spatula electrode

3.4 Numerical Model

A finite element (FE) model was also developed, initially limited and validated respect to the case of the ESST1, then enlarged to other scalpels. This electrode was chosen since more measurements were available for validation.

Starting from the original shape (as evident from scalpel's image), a simplified CAD geometry was produced. A spherical rounding of the end was introduced to dampen the 'tip effect' (Figure 15a).

The discretization was performed by Ansys WB using three-dimensional (3D) tetra solids Fes with a total of 766108 nodes and 544561 elements. The algorithm created a mesh entirely composed of 10-node tetrahedra focused on surfaces and interfaces to give a more realistic shape and outline (Figure 15b).

The applied conditions are related to the temperature only. In fact, the internal heating of the electrode linked to the Joule effect was considered negligible (at this first stage of modeling), also supported by preliminary measurements (closed circuit) which showed marginal variations in the temperature of the electrode. A sphere was used to represent the plasma from which the electrode was heated by heat transfer. Specifically, the electrode was designed as immersed in a plasma bubble, placed at 1,800 °C, which wrapped it uniformly for 0.5 mm. At 0.5 mm outside the sphere, therefore equal to 1 mm from the extremity, equivalent to point A, a condition of $T = 1,620^{\circ}\text{C}$ was set. Three further temperatures were then applied, according to the measures (Figure 15c).

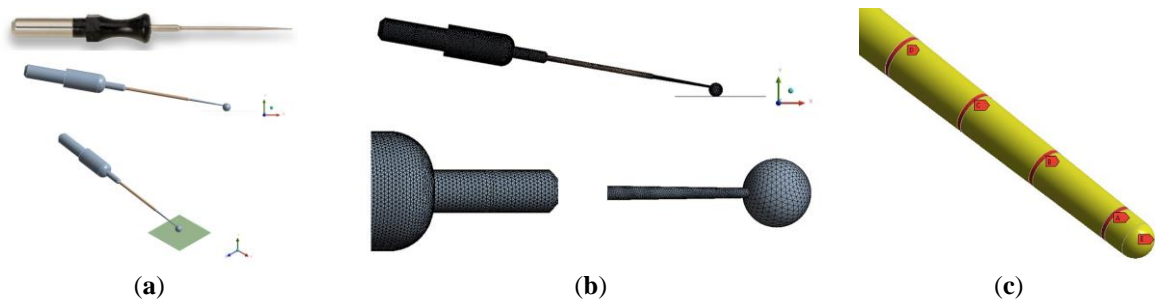


Figure 15. Different phases of the numerical modelling: (a) CAD geometrical modeling and application of a plasma 'bubble'; (b) finite element discretization; (c) application of temperature external conditions

The numerical computation allowed to estimate the:

- temperature at each point of the electrode (Figure 16)
- heat emissions (W/mm) in the transverse (Y) and longitudinal (X) direction

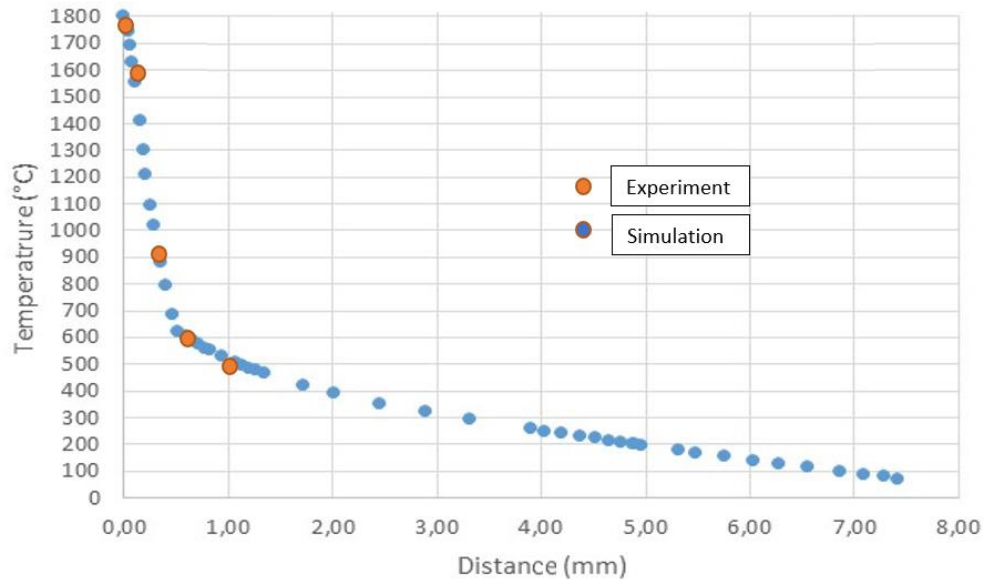


Figure 16. Reconstruction of the temperature trend in the electrode starting from the measured values

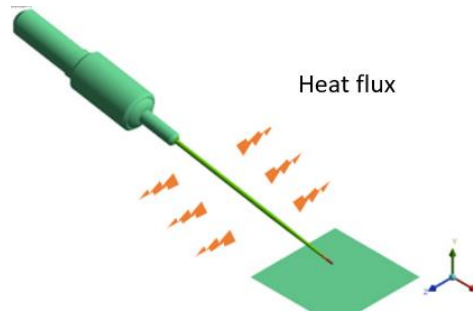


Figure 17. Representation of heat flux as a way to estimate the impact on surrounding tissues

The transverse heat flux, better than temperature, could offer a first estimation of the thermal stress of the tissue. The temperature, in fact, simply represents the state of agitation of the molecules inside the electrodes. However, the damage to the tissue is not directly caused by the state of agitation of such molecules. Instead, it is connected to the portion of energy that is transferred from the electrode to the tissue. In these terms, thanks to the model, it was possible to estimate the highest quantity of energy transferable to the tissue. Later, introducing the physical characteristics of the tissue, it will be maybe possible to have an approximate idea of how much energy can be absorbed before a damage. Then, the radial heat flow represents the energy that is transmitted to the outside and that can be intercepted by the tissue (Figure 17).

Finally, thanks to the simulation, it was easy to investigate the effect of Teflon through a layering of materials (Figure 18).

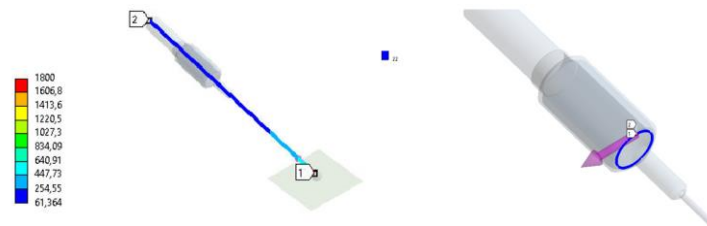


Figure 18. Numerical discretization as a way to estimate temperatures in multi-material electrodes

3.5 Further Considerations

This work, as said, aimed to evolve cold plasma technology with the target of developing new devices for high precision human and veterinary surgery. With such a scope, an accurate control on temperatures will foster the use of cold plasma in neurosurgery and on the central nervous system. Moreover, the development of specific probes will make it possible to bring this new interventional technique to endoscopy and laparoscopy operations, hitherto substantially excluded compared to the advantages offered by cold plasma. Less invasiveness, reduction of pain during and after, rapid healing, reduced healing times, better functional and aesthetic result will be some of the benefits offered by the new plasma cutting, more precise and with effective hemostasis. Surgical scalpels and probes, very different in function from what has been in circulation so far, will thus expand traditional electrosurgery, allowing the advantages of cold plasma to be extended to other interventional fields as well.

All this is possible only when the thermal behavior of the electrodes can be fully understood. For example, the knowledge of which are the areas of the electrode that, despite being at high temperatures, are likely to come into contact with the patient during the surgery, can help to decide where to apply Teflon as a thermal insulation element. On the contrary, the reduced risk of contact can lead to the decision to leave the electrode uncovered in order to favor thermal dissipation in the environment. Similarly, thanks to the knowledge of the temperature of the various electrodes, the intervention procedures can be modified to make it more efficient and less invasive.

For such a general purpose, the experimental measurements were also used for developing a numerical model able to predict the temperature profiles. The behavior in air of plasma flows represents a problem of difficult solution and still open despite the many studies. Far from proposing a general and exact solution, in this study the sole objective was to develop a thermodynamic model of heat diffusion capable of predicting the temperature distributions inside the electrode (made of steel, with additional parts in Teflon and tungsten sometimes). For this purpose, many simplifications have been introduced while achieving results in line with the measurements.

The model allowed a fast and fairly accurate comparison of different design hypotheses with respect to geometric changes and in the materials of the electrodes.

4. Conclusions

Experimental measurements made it possible to detect the temperature profiles that emerged in the 4 most representative electrodes using an innovative air plasma technology. For the purpose, temperature, probes detecting temperature, voltage and current were used, as well as alignment equipment and various calibration procedures. Considering the experimental evidence, respect to the air plasma process under investigation, it is possible to report that:

- The process is fully repetitive.
- The plasma appears to be stable at temperatures around 1,800-1,860°C.
- The conditions are strongly modified by the electrode geometry.
- The electrode heats up linearly for a first stretch and then quickly reaches equilibrium.
- The effects of the thermodynamic transition (of the order of 10 seconds) can be neglected.
- Temperatures drop rapidly as you move away from the plasma area.
- Teflon markedly modifies the thermal behavior of the electrode.
- The power selector does not significantly change the temperature profile.
- Measurements on tissue cannot be obtained with a similar method, nor with fiber optic sensors.
- A numerical model would be able to accurately describe many of the emerging phenomena.
- Through this model it would be possible to reconstruct information impossible to measure.

Author Contributions

Conceptualization, C.F.; methodology, C.F. and M.A.; software, A.P.; validation, C.F. and F.C.; formal analysis, C.F.; investigation, C.F., M.A., F.C. and A.P.; resources, C.F.; data curation, C.F. and A.P.; writing—original draft preparation, C.F.; writing—review and editing, C.F. and F.C.; visualization, C.F.; supervision, C.F.; project administration, M.A.; funding acquisition, M.A. All authors have read and agreed to the published version of the manuscript.

Funding

This work is co-funded by MEDITECH Competence Center (project acronym: ‘AirplasmaEVO’).

Data Availability

The data supporting our research results may be released upon request.

Acknowledgements

The authors wish to thank OTECH Industry S.r.l., in the persons of Franco Pavignano and Loris Ghione, for providing the Oneyonis® air plasma device together with several valid recommendations for its optimal use.

Conflicts of Interest

The authors declare no conflict of interest.

References

- [1] S. Saraf and R. Parihar, “Sushruta: The first Plastic Surgeon in 600 B.C.,” *Internet J. Plast Surg.*, vol. 4, no. 2, pp. 1-7, 2006.
- [2] V. W. Green, “Surgery, sterilization and sterility,” *J. Healthc Mater Manage*, vol. 11, no. 2, pp. 48-52, 1993.
- [3] N. M. Greene, “Anesthesia and the development of surgery (1846-1896),” *Anesth Analg.*, vol. 58, no. 1, pp. 5-12, 1979. <https://doi.org/10.1213/00000539-197901000-00003>.
- [4] G. Rispoli and C. Rispoli, “History of haemostasis in surgery,” *Med Secoli.*, vol. 17, no. 3, pp. 811-821, 2005.
- [5] M. Ramachandran and J. K. Aronson, “John Marshall's first description of surgical electrocautery,” *J. R Soc. Med.*, vol. 104, no. 9, pp. 355-360, 2017. <https://doi.org/10.1258/jrsm.2011.11k028>.
- [6] W. D. Rappaport, G. C. Hunter, R. Allen, S. Lick, A. Halldorsson, T. Chvapil, M. Holcomb, and M. Chvapil, “Effect of electrocautery on wound healing in midline laparotomy incisions,” *Am J. Surg.*, vol. 160, no. 6, pp. 618-620, 1990. [https://doi.org/10.1016/s0002-9610\(05\)80757-3](https://doi.org/10.1016/s0002-9610(05)80757-3).
- [7] P. U. Abdul Wahab, M. Madhulaxmi, P. Senthilnathan, M. R. Muthusekhar, Y. Vohra, and R. P. Abhinav, “Scalpel versus diathermy in wound healing after mucosal incisions: A split-mouth study,” *J. Oral Maxil Surg.*, vol. 76, no. 6, pp. 1160-1164, 2017. <https://doi.org/10.1016/j.joms.2017.12.020>.

- [8] D. S. Choy, "History of lasers in medicine," *Thorac Cardiovasc Surg.*, vol. 36, no. 2, pp. 114-117, 2007. <https://doi.org/10.1055/s-2007-1022985>.
- [9] H. D. Sandel and S. W. Perkins, "CO₂ laser resurfacing: Still a good treatment," *Aesthet Surg. J.*, vol. 28, no. 4, pp. 456-462, 2008. <https://doi.org/10.1016/j.asj.2008.05.001>.
- [10] V. C. Wright, "Laser surgery: Using the carbon dioxide laser," *Can Med Assoc J.*, vol. 126, no. 9, pp. 1035-1039, 1982.
- [11] D. K. Dutta and I. Dutta, "The harmonic scalpel," *J. Obstet Gynaecol India*, vol. 66, no. 3, pp. 209-210, 2016. <https://doi.org/10.1007/s13224-016-0850-x>.
- [12] B. K. Sah, J. J. Yang, G. T. Yang, and X. W. Zhang, "Clinical uses of ligasure vessel sealing system (LVSS) in surgery," *J. Nanjing Med Univ.*, vol. 22, no. 2, pp. 102-106, 2008. [https://doi.org/10.1016/S1007-4376\(08\)60021-0](https://doi.org/10.1016/S1007-4376(08)60021-0).
- [13] V. C. Karande, "LigaSure 5-mm blunt tip laparoscopic instrument," *J. Obstet Gynaecol India.*, vol. 65, no. 5, pp. 350-352, 2015. <https://doi.org/10.1007/s13224-015-0745-2>.
- [14] U. Kogelschatz, "Atmospheric-pressure plasma technology," *Plasma Phys. Contr F.*, vol. 46, no. 12, Article ID: B63, 2004. <https://doi.org/10.1088/0741-3335/46/12B/006>.
- [15] M. Domonkos, P. Tichá, J. Trejbal, and P. Demo, "Applications of cold atmospheric pressure plasma technology in medicine, agriculture and food industry," *Appl. Sci.*, vol. 11, no. 11, Article ID: 4809, 2021. <https://doi.org/10.3390/app11114809>.
- [16] S. A. Loh, G. A. Carlson, E. I. Chang, E. Huang, D. Palanker, and G. C. Gurtner, "Comparative healing of surgical incisions created by the PEAK PlasmaBlade, conventional electrosurgery, and a scalpel," *Plast Reconstr Surg.*, vol. 124, no. 6, pp. 1849-1859, 2009. <https://doi.org/10.1097/PRS.0b013e3181bcee87>.
- [17] K. Peprah and C. Spry, "Pulsed Electron Avalanche Knife (PEAK) PlasmaBlade versus traditional electrocautery for surgery: A review of clinical effectiveness and cost-effectiveness," *Can Agency Drugs Technol. Health*, vol. 2019, Article ID: 31693325, 2019.
- [18] "Medical Devices with Airplasma® Technology," Otechindustry, 2022, <http://www.otechindustry.it/en/airplasma/patent>.
- [19] "Improved tissue healing due to less thermal damage," OTECH Industry, 2022, <https://www.oneyonis.it/en/device/>.
- [20] "Onemytis," Onemytis, 2022, <http://www.onemytis.it/en/>.
- [21] A. Vezzoni, M. De Lorenzi, and L. Vezzoni, "Clinical use of a new plasma device," *Veterinaria*, vol. 30, no. 4, pp. 1-8, 2016.
- [22] L. Lacitignola, S. Desantis, G. Izzo, F. Staffieri, R. Rossi, L. Resta, and A. Crovace, "Comparative morphological effects of cold-blade, electrosurgical, and plasma scalpels on dog skin," *Vet Sci.*, vol. 7, no. 1, pp. 8-8, 2020. <https://doi.org/10.3390/vetsci7010008>.

Appendix

N°	Electrode	Point	Intensity (%)	(A)	Time (s)	Temperature (°C)	Plateau
1	ESST1	A	100	2.80	6	899	YES
2	ESST1	A	100	2.90	6	777	YES
3	ESST1	A	100		8	750	YES
4	ESST1	A	100		8	787	YES
5	ESST1	A	100		8	726	YES
6	ESST1	A	100	2.62	8	1764	YES
7	ESST1	A	100		8	1800*	YES
8	ESST1	A	100	2.62	8	1800*	YES
9	ESST1	A	100		9	1800*	YES
10	ESST1	B	100		8	1085	YES
11	ESST1	B	100		8	983	YES
12	ESST1	B	100	2.42	8	930	YES
13	ESST1	C	100	2.46	8	547	YES
14	ESST1	C	100	2.62	8	589	YES
15	ESST1	C	100	2.58	11	636	YES
16	ESST1	C	100	2.45	10	647	YES
17	ESST1	C	100	2.46	10	627	YES
18	ESST1	C	100	2.52	11	662	YES
19	ESST1	C	70	2.36	11	648	YES
20	ESST1	C	70	2.45	11	666	YES
21	ESST1	C	70	2.29	11	676	YES
22	ESST1	C	40	2.35	11	640	YES
23	ESST1	C	40	2.27	12	649	YES
24	ESST1	C	40	2.25	12	638	YES
25	ESST1	D	100	2.32	11	566	YES

26	ESST1	D	100	2.30	13	581	YES
27	ESST1	D	100	2.24	13	582	YES
28	ESST1	D	70	2.32	13	576	YES
29	ESST1	D	70	2.27	13	575	YES
30	ESST1	D	70	2.30	13	567	YES
31	ESST1	D	40	2.20	13	555	YES
32	ESST1	D	40	2.25	13	555	YES
33	ESST1	D	40	2.25	13	542	YES
34	ESTT1	A	100	2.47	8	1163	YES
35	ESTT1	A	100	2.55	6	1230	YES
36	ESTT1	A	100	2.54	7	1241	YES
37	ESTT1	A	100	2.58	6	1258	YES
38	ESTT1	A	100	2.51	6	1238	YES
39	ESTT1	B	100	2.85	6	640	YES
40	ESTT1	B	100	2.59	7	624	YES
41	ESTT1	B	100	2.53	6	665	YES
42	ESTT1	B	100	2.57	6	638	YES
43	ESTT1	B	70	2.63	6	647	YES
44	ESTT1	B	70	2.71	6	650	YES
45	ESTT1	B	70	2.71	6	663	YES
46	ESTT1	B	40	2.84	6	619	YES
47	ESTT1	B	40	2.93	6	633	YES
48	ESTT1	B	40	2.73	6	628	YES
49	ESSP4	A	100	2.15	13	960	YES
50	ESSP4	A	100	2.12	22	1048	NO
51	ESSP4	A	100	2.17	22	1032	NO
52	ESSP4	A	70	2.20	22	1021	NO
53	ESSP4	A	40	2.26	22	1017	NO
54	ESSP4	B	100	2.22	22	590	NO
55	ESSP4	B	100	2.10	22	618	NO
56	ESSP4	B	100	2.23	22	618	NO
57	ESSP4	B	70	2.19	22	607	NO
58	ESSP4	B	40	2.21	22	600	NO
59	ESSP4	C	100	2.20	25	373	NO
60	ESSH3	A	100	1.80	22	619	NO
61	ESSH3	A	100	1.95	22	643	NO
62	ESSH3	A	100	1.92	22	641	NO
63	ESSH3	A	70	1.80	22	645	NO
64	ESSH3	A	40	1.82	22	643	NO
65	ESTT1	B	100			289	NO
Values				57.00		65	49
average				2.39		741	
st.dev				0.27		252	